Nonlinear evolution of thermal self-focusing instability in ionospheric modifications at high latitudes: Aspect angle dependence

N. A. Gondarenko,[1] S. L. Ossakow,[2] and G. M. Milikh[3]

Received 13 February 2006; revised 4 July 2006; accepted 17 July 2006; published 26 August 2006.

[1] A first simulation study for the nonlinear evolution of the thermal self-focusing instability at high latitudes to examine the dependence of the nonlinear effects on the direction of the heater beam is presented. We demonstrate that due to a local heating of the *F* region anisotropic plasma, field-aligned bunch-scale structures with a strong enhancement of the electron temperature and negative density perturbations inside these structures are developed. The electron temperature increases up to more than 200% of the background when the incident beam is near the magnetic zenith, as observed in the heating experiment at the EISCAT high-latitude facility (Rietveld et al., 2003). The values of the simulated electron temperature enhancements show a strong dependence on the heater beam direction that is in very good agreement with the EISCAT observations. **Citation:** Gondarenko, N. A., S. L. Ossakow, and G. M. Milikh (2006), Nonlinear evolution of thermal self-focusing instability in ionospheric modifications at high latitudes: Aspect angle dependence, *Geophys. Res. Lett.*, *33*, L16104, doi:10.1029/2006GL025916.

1. Introduction

[2] The current understanding of the heating effects at high latitudes is rapidly progressing due to better communication of results from recent observations, theories, and modelling. Recent observations at high latitudes near Tromsø [*Rietveld et al.*, 2003], the only HF heating facility equipped with an incoherent scatter radar, show that powerful radio emission directed along the magnetic field lines causes a strong enhancement of electron temperature. *Rietveld et al.* [2003] are the first to directly measure the electron temperature enhancement in this region.

[3] The dependence of the HF heating effects on the direction of the heater beam were first stated theoretically by *Gurevich et al.* [1999]. The observations of the unexplained southward airglow displacement were first reported at Tromsø by *Kosch et al.* [2000]. At the HAARP heating facility, *Pedersen and Carlson* [2001] and *Pedersen et al.* [2003] observed a strong airglow enhancement toward magnetic zenith. The comprehensive analysis of the EISCAT and HAARP observations [*Gurevich et al.*, 2001] resulted in the development of a theory of the magnetic zenith effects in ionospheric modifications [*Gurevich et al.*, 2002]. *Gurevich et al.* [2001, 2002] demonstrated that a strong amplification of modification effects when a powerful beam is directed to magnetic zenith is caused by self-focusing of the pump wave on striations. The field-aligned striations are originated in the vicinity of the ordinary wave reflection point, where weak seed irregularities naturally existed or artificially created are amplified by the self-focusing instability (SFI) of a plasma wave [*Vaskov et al.*, 1981]. In time, these irregularities extend along the magnetic field lines upward and downward. The 10-m scale irregularities with ~6% depletion depth have been measured by *Kelley et al.* [1995] in the midlatitude experiments. When the average electron density is reduced due to the negative density perturbations inside of a large number of striations, self-focusing on striations takes place that leads to the formation of soliton-like nonlinear structures, bunches of striations aligned along the magnetic field [*Gurevich et al.*, 1998].

[4] The observations of kilometer-scale density irregularities attributed to the SFI by *Perkins and Valeo* [1974] have been made with a scintillation technique by *Basu et al.* [1987] and radar scattering by *Duncan and Behnke* [1978] and *Farley et al.* [1983]. Recently, 0.5–2 km scale field-aligned structures have been obtained in the HAARP heating experiment [*Djuth et al.*, 2006] where a dramatic increase in the number of irregularities for the field-aligned transmissions has been observed.

[5] *Rietveld et al.* [2003] presented data from a nighttime experiment on October 7, 1999 when both the HF-pump beam and the diagnostic radar beams were scanned electronically in elevation between magnetic field-aligned and vertical directions: 6° (Spitze angle), 0° (vertical direction), and 12° (field-aligned direction). The strongest heating effects, large electron temperature increases up to 3000 K above the background, have been measured in the field-aligned direction. The electron temperature increases become weaker for the vertical and Spitze positions of the heater beam.

[6] The objective of this paper is to demonstrate, using simulation results of the nonlinear evolution of the thermal SFI, that the heating effects are amplified when the heater beam is incident along the magnetic field line. We show for the first time in numerical simulations the dependence of the simulated electron temperature enhancements on the heater beam direction that is in very good agreement with recent observations at EISCAT by *Rietveld et al.* [2003].

2. Simulation Results

[7] Recently, *Gondarenko et al.* [2005] have demonstrated with the 2-D numerical model for the thermal SFI that irregularities generated and developed due to a local heating

[1]Institute for Research in Electronics and Applied Physics, University of Maryland, College Park, Maryland, USA.
[2]Plasma Physics Division, Naval Research Laboratory, Washington, D. C., USA.
[3]Department of Astronomy, University of Maryland, College Park, Maryland, USA.

0094-8276/06/2006GL025916

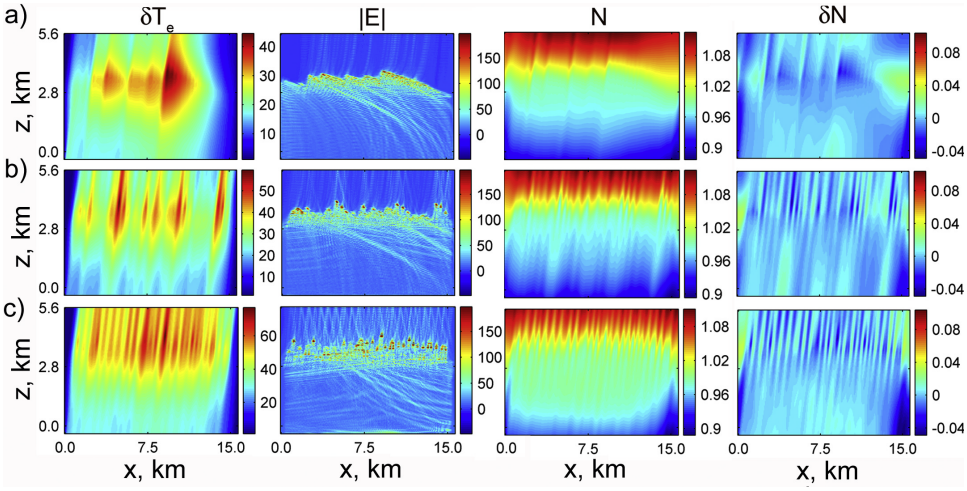

Figure 1. Contours of δT_e, $|E|$, $N = N_0 + \delta N_e$, and δN_e at $t \sim 43$ ms for (a) $\gamma = 0°$, (b) $\gamma = 6°$, and (c) $\gamma = 12°$.

of the anisotropic ionosphere plasma are (4–10%) density depletions with a strong enhancement of electron temperature inside the depletions ($T_e \approx 2\ T_{e0}$) elongated along the magnetic field lines. The characteristics of the simulated density and temperature irregularities are in a good agreement with the theories by *Gurevich et al.* [1995, 1998, 2002]. In the 2D numerical model, the full-wave model [*Ginzburg*, 1970] is coupled with density and temperature evolution equations to study the full nonlinear, self-consistent development of the thermal self-focusing instability [*Gondarenko et al.*, 2005].

[8] In the coordinate system we choose, the vertical z axis is along the density gradient, x points to the south direction, and the external constant geomagnetic field $H^{(0)}$ is in the xz-plane (the plane of magnetic meridian). The magnetic field makes an angle α with the z axis, $\alpha = 13°$. When the heater beam is tilted to the magnetic field, we use $\gamma = 12°$ and $\gamma = 6°$ for the field-aligned propagation and propagation at the Spitze angle. Here γ is the angle between the wave-propagation direction and the vertical. The sets of parameters chosen for these simulations are for the F region at the EISCAT HF facility near Tromsø [*Rietveld et al.*, 2003]. We use O-mode heating with the pump wave frequency $\omega = 2\pi \cdot 4.544$ MHz, the electron cyclotron frequency $\Omega_e = 2\pi \cdot 1.3$ MHz, the effective electron collision frequency $\nu_{e0} = 10^3$ s^{-1}, and the background electron temperature $T_{e0} = 1300$ K. For the EISCAT heater ERP $P_0 = 205$ MW and distance $R = 285$ km, the wave amplitude is $E_0 \simeq 4.7\sqrt{P_0}/R \simeq 0.24$ V/m (without taking into account the E-region absorption).

[9] In our simulations, the box sizes are $L_x = 15.9$ km and $L_z = 5.96$ km in the x and z directions, respectively. The simulations were performed on a grid [256, 512] with grid sizes $\Delta x = 63$ m, $\Delta z = 11.6$ m, so that there are about 6 points per wavelength in the z direction. The intensity of the incident radiation is given at the lower boundary where the amplitude and phase of the upward going wave are specified [*Gondarenko et al.*, 2004]. For the temperature and density at the lower and upper boundaries, we set the gradient of the perturbed temperature and density along the magnetic field lines to be zero. In the x direction, we use a periodic boundary condition for the density. Our initial conditions are the following: the temperature is uniform in the box, the density has linear variation in z, $N(z) = 1 + (z - z_c)/L$, where $L = 30$ km is the scalelength of the density

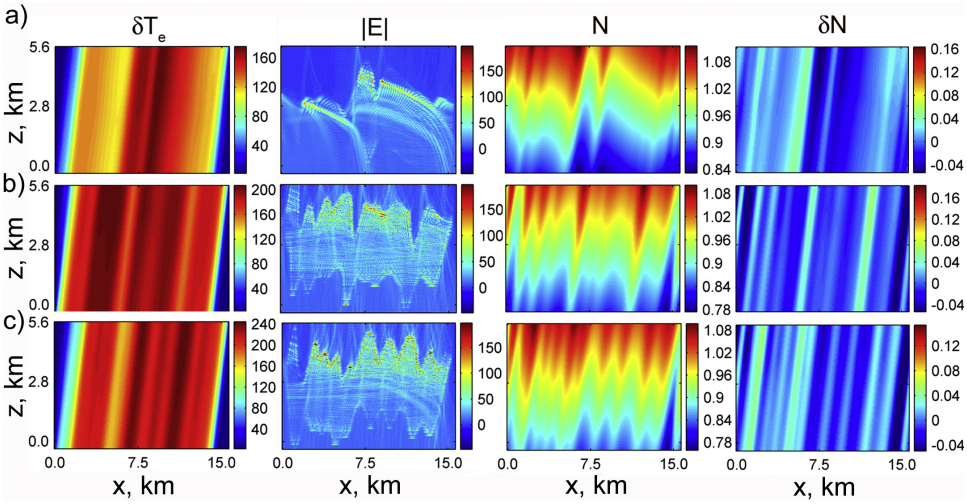

Figure 2. Contours of δT_e, $|E|$, $N = N_0 + \delta N_e$, and δN_e at $t \sim 500$ ms for (a) $\gamma = 0°$, (b) $\gamma = 6°$, and (c) $\gamma = 12°$.

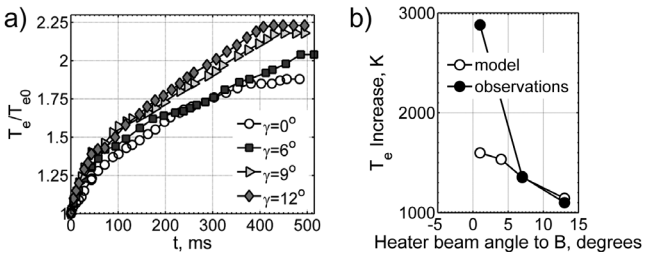

Figure 3. (a) Time evolution of maximal T_e/T_{e0}, (b) Electron temperature increase vs heater beam angle to the magnetic field.

inhomogeneity and z_c is the critical layer ($V = \omega_{pe}^2/\omega^2 = 1$) at which the local electron plasma frequency ω_{pe} matches the given wave frequency. We initialize the perturbed density in the small region in z ($\sim$50 m above and below the critical layer) as a superposition of 8 sine modes in the x direction with random phases and overall amplitude of $\sim$1%.

[10] In Figures 1a–1c we show contours of the normalized electron temperature fluctuations δT_e, the amplitude of the total electric field $|E|$, the density $N = N_0 + \delta N_e$, and the density fluctuations $\delta N_e = N - \langle N \rangle_x$ at $t \sim 43$ ms for various angles of incidence: vertical ($\gamma = 0°$), Spitze angle ($\gamma = 6°$), and in field-aligned direction ($\gamma = 12°$), respectively. Here $T_e/T_{e0} = 1 + \delta T_e/(z_0\omega/c)^2$, where z_0 is the Airy length and c is the velocity of light. The electric field plot in Figure 1a demonstrates the Airy pattern formed by the reflection of the O mode. One can see that the swelling (an increase in the field strength) due to the effect of the geomagnetic field is significant [*Gondarenko et al.*, 2003]. At the resonance layer $V_\infty = (1 - U)/(1 - U\cos^2\alpha)$, $U = Y^2 = (\Omega_e/\omega)^2$, due to the presence of the small-scale density irregularities δN_e, the O mode can be transformed into the second branch, the extraordinary (X) mode, which in the ionospheric context is referred to as the Z mode. The reflected Z mode propagates toward the plasma resonance region V_∞ where it is converted into an electrostatic mode. In this case the irregularities serve as resonators excited by the ordinary wave. As the result of these processes the wave amplitudes near $V = 1$ are intensified. In Figures 1a–1c at the localized regions near $z \sim 2.8$ km, the field amplitude increases by a factor of 25, 36, and 45, respectively. One can observe a modulation in the electric field pattern, wavy density structures, and upward shifts of the reflection points, which is higher for the waves of higher intensity, here for the incidence in the field-aligned direction.

[11] The presence of weak density irregularities in the narrow region near $V = 1$ results in the excitation of the SFI instability. The nonlinearity associated with the changes of the refractive index causes a stratification of the beam, modulation in the wave field, and perturbation of the plasma density. During the nonlinear evolution of the SFI instability, the reflection point of the ordinary wave is shifted upward with decreasing electron concentration and the bunching of striations is observed. It has been demonstrated by *Gurevich* [1965] that the reflection point shifts upward into the interior of the plasma when the electron concentration decreases under the influence of the alternating electric field.

[12] The δT_e contours in Figures 1a–1c show that there are about 5, 7, and 17 field-aligned structures, respectively. At this time, the waves of higher intensity heat the plasma at the localized regions, the temperature fluctuations δT_e increase while the plasma density is depleted, $N - N_0 < 0$. Temperature and density perturbations become elongated in the direction of the magnetic field due to transport processes. For the incidence in the field-aligned direction, the localized regions of the perturbed temperature diffuse mostly above the original O-mode reflection layer along the magnetic zenith direction. The amplitudes of δT_e are higher when compared with those for the normal and Spitze incidence cases. The diffusion of heat into the overdense plasma reduces the density in the region above the critical layer, allowing the heater wave to propagate upward, that results in shifts of the critical layers.

[13] As time progresses, the density and temperature perturbations evolve into larger structures (Figures 2a–2c, $t \sim 500$ ms) with transverse scale sizes of $\sim$1–3 km. One can see that nonlinear development of the thermal SFI results in formation of the field-aligned bunch-scale structures. The maximal depth of the depletions is $\sim$4–5%. The electron temperature inside the bunches of striations is $T_e \sim 1.87\ T_{e0}$ for normal incidence and it is maximal $T_e \sim 2.25\ T_{e0}$ for the field-aligned beam propagation.

[14] In Figure 3a we show the time evolution of the maximal T_e/T_{e0} inside the bunches of striations for the cases $\gamma = 0°$, $6°$, $9°$, and $12°$. The reduction in growth of temperature perturbations is due to the fact that T_e is inversely proportional to the characteristic scale of the transport process along the field lines as discussed by *Gondarenko et al.* [2005].

[15] In Figure 3b we present the simulated and observed dependencies of the T_e enhancement on the angle of the heater beam to the magnetic field. For the normal and Spitze angle incidences, the simulated values of the T_e increase are $\sim$1130 K and 1350 K that is in very good agreement with recent observations at EISCAT by *Rietveld et al.* [2003]. For the Spitze angle incidence, the T_e increase drops to 1350 K that is only $\sim$275 K lower than the field-aligned value.

[16] In the EISCAT observations, the heating was the strongest in the field-aligned direction (3000 K above background) while the simulated field-aligned value reaches only 1625 K. Note that in the simulations for magnetic zenith propagation, irregularities with smaller scales occur so higher resolution is required. The time for the development of the nonlinear thermal SFI is only half a second, during which the electric field perturbations propagate up to the top boundary, while in the EISCAT experiment the operation cycle is 8 min on followed by 4 min off. The restrictions on the sizes of the computational box are imposed by the requirement to resolve scales in the localized mode-conversion regions of the wave patterns. Thus with higher resolutions and longer heating, one can expect a larger enhancement of T_e for field-aligned propagation. Also note that within our model for wave propagation in a "cold" inhomogeneous magnetized plasma [*Ginzburg*, 1970], a singularity at the plasma resonance region is resolved by taking into account the effective electron collision frequency ν_{eff}. Considering the "warm" plasma effects in the dielectric tensor will allow one to account for various types of instabilities which may also contribute to the T_e increase.

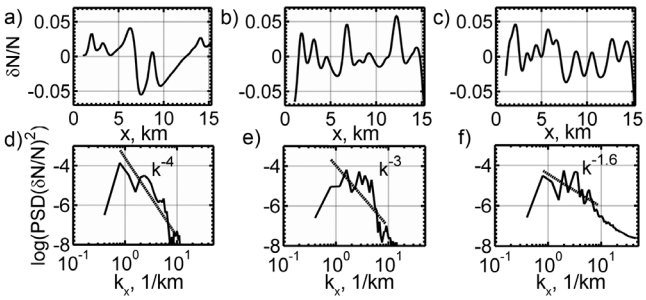

Figure 4. Amplitudes and power spectra of $\Delta N_e/N$ for (a and d) $\gamma = 0°$, (b and e) $\gamma = 6°$, and (c and f) $\gamma = 12°$.

[17] Figure 4 shows the $\Delta N/N$ fluctuations with the corresponding spectra for normal, Spitze, and field-aligned incidences. The $\Delta N/N$ spectra have been computed in the interval $k_x \in [0.395, 44.6]$ km^{-1} ($\sim$15.9–0.14 km in scale size) with the spectral slopes determined in the interval $\sim$7.96–0.72 km in scale size. Here one can see that the spectral slope is shallower when the pump beam is directed to the magnetic zenith ($\gamma = 12°$) while the slope is steeper for normal incidence. The spectral characteristics of the simulated $\Delta N/N$ are similar to those observed in the mid-latitude experiments at the SURA HF facility [*Tereshchenko et al.*, 2004]. We use the values of the power spectral density (PSD) -5 ± 0.2 as an indicator for the irregularities level in the spectra. We identify the dominant scale size of the structures as an average of scale sizes corresponding to local peaks with the values of PSD larger than -5 ± 0.2. In Figure 4d, a local maximum in the spectrum at $k \sim 2.37$ km^{-1} which corresponds to the wavelength of $\sim$2.65 km can be interpreted as the dominant scale size, the scale size of the depletions. At wave numbers higher than that, the fluctuation spectrum falls rapidly, which is associated with the finite gradient in the edges of striations. For the Spitze and field-aligned incidences (Figures 4e and 4f), the dominant scale size decreases to 1.8 and 1.6 km, respectively. The peaks in the larger scale parts of the spectra (Figures 4d–4f) correspond to the separation scale between the bunch-scale structures where $\delta N_e/N > 0$.

[18] In conclusion, we have demonstrated that the strongest heating effects observed in the field-aligned direction in the heating experiment [*Rietveld et al.*, 2003] are due to the nonlinear development of the thermal SFI instabilities. The simulation results demonstrate that due to a local heating of the *F* region anisotropic plasma, field-aligned bunch-scale density depletions with a strong enhancement of the electron temperature and negative density perturbations inside the depletions are developed. The electron temperature increases up to more than 200% of the background when the incident beam is near the magnetic zenith. The values of the simulated electron temperature enhancements show a strong dependence on the heater beam direction that is in very good agreement with recent EISCAT observations. The spectral characteristics of the simulated $\delta N/N$ are similar to those obtained in the midlatitude simulations by *Gondarenko et al.* [2005].

[19] **Acknowledgment.** This research was supported by the Office of Naval Research and in part by the HAARP program.

References

Basu, S., S. Basu, P. Stubbe, H. Kopka, and J. Waaramaa (1987), Daytime scintillations induced by high-power HF waves at Tromso, Norway, *J. Geophys. Res.*, *92*, 11,149.

Djuth, F. T., B. W. Reinisch, D. F. Kitrosser, J. H. Elder, A. L. Snyder, and G. S. Sales (2006), Imaging HF-induced large-scale irregularities above HAARP, *Geophys. Res. Lett.*, *33*, L04107, doi:10.1029/2005GL024536.

Duncan, L. M., and R. A. Behnke (1978), Observations of self-focusing electromagnetic waves in the ionosphere, *Phys. Rev. Lett.*, *41*, 998.

Farley, D. T., C. LaHoz, and J. A. Fejer (1983), Studies of the self-focusing instability at Arecibo, *J. Geophys. Res.*, *88*, 2093.

Ginzburg, V. L. (1970), *The Propagation of Electromagnetic Waves in Plasmas*, Pergamon Press., Oxford, New York.

Gondarenko, N. A., P. N. Guzdar, S. L. Ossakow, and P. A. Bernhardt (2003), Linear mode conversion in inhomogeneous magnetized plasmas during ionospheric modification by HF radio waves, *J. Geophys. Res.*, *108*(A12), 1470, doi:10.1029/2003JA009985.

Gondarenko, N. A., P. N. Guzdar, S. L. Ossakow, and P. A. Bernhardt (2004), Perfectly matched layers for radio wave propagation in inhomogeneous magnetized plasmas, *J. Comp. Phys.*, *194*, 481.

Gondarenko, N. A., S. L. Ossakow, and G. M. Milikh (2005), Generation and evolution of density irregularities due to self-focusing in ionospheric modifications, *J. Geophys. Res.*, *110*, A09304, doi:10.1029/2005JA011142.

Gurevich, A. V. (1965), Penetration of an electromagnetic wave into a plasma with account of non-linearity, *Sov. Phys. JETP, Engl. Transl.*, *21*, 462.

Gurevich, A. V., A. V. Lukyanov, and K. P. Zybin (1995), Stationary state of isolated striations developed during ionospheric modification, *Phys. Lett. A*, *206*, 247.

Gurevich, A. V., T. Hagfors, H. Carlson, A. N. Karashtin, and K. Zybin (1998), Self-oscillations and bunching of striations in ionospheric modifications, *Phys. Lett. A*, *239*, 385.

Gurevich, A. V., H. Carlson, M. Kelley, T. Hagfors, A. Karashtin, and K. P. Zybin (1999), Nonlinear structuring of the ionosphere modified by powerful radio waves at low latitudes, *Phys. Lett. A*, *251*, 311.

Gurevich, A. V., H. Carlson, and K. P. Zybin (2001), Nonlinear structuring and southward shift of a strongly heated region in ionospheric modification, *Phys. Lett. A*, *288*, 231.

Gurevich, A. V., K. P. Zybin, H. C. Carlson, and T. Pedersen (2002), Magnetic zenith effect in ionospheric modifications, *Phys. Letts. A*, *305*, 264.

Kelley, M. C., T. L. Arce, J. Saloway, M. Sulzer, T. Armstrong, M. Carter, and L. Duncan (1995), Density depletions at the 10-m scale induced by the Arecibo heater, *J. Geophys. Res.*, *100*, 367.

Kosch, M. J., M. T. Rietveld, T. Hagfors, and T. B. Leyser (2000), High-latitude HF-induced airglow displaced equatorwards of the pump beam, *Geophys. Res. Lett.*, *27*, 2817.

Pedersen, T. R., and H. C. Carlson (2001), First observations of HF heater-produced airglow at the High Frequency Active Auroral Research Program facility: Thermal excitation and spatial structuring, *Radio Sci.*, *36*, 1013.

Pedersen, T. R., M. McCarrick, E. Gerken, C. Selcher, D. Sentman, H. C. Carlson, and A. Gurevich (2003), Magnetic zenith enhancement of HF radio-induced airglow production at HAARP, *Geophys. Res. Lett.*, *30*(4), 1169, doi:10.1029/2002GL016096.

Perkins, F. W., and E. J. Valeo (1974), Thermal self-focusing of electromagnetic waves in plasmas, *Phys. Rev. Lett.*, *32*, 1234.

Rietveld, M. T., M. J. Kosch, N. F. Blagoveshchenskaya, V. A. Kornienko, T. B. Leyser, and T. K. Yeoman (2003), Ionospheric electron heating, optical emissions, and striations induced by powerful HF radio waves at high latitudes: Aspect angle dependence, *J. Geophys. Res.*, *108*(A4), 1141, doi:10.1029/2002JA009543.

Tereshchenko, E. D., B. Z. Khudukon, A. V. Gurevich, K. P. Zybin, V. L. Frolov, E. N. Myasnikov, N. V. Muravieva, and H. C. Carlson (2004), Radio tomography and scintillation studies of ionospheric electron density modification caused by a powerful HF-wave and magnetic zenith effect at mid-latitudes, *Phys. Lett. A*, *325*, 381.

Vaskov, V. V., A. V. Gurevich, and A. N. Karashtin (1981), Thermal self-focusing instability of plasma waves near resonance, *Geomagn. Aeron.*, *21*, 724.

N. A. Gondarenko, IREAP, University of Maryland, College Park, MD 20742, USA. (ngondare@umd.edu)

G. M. Milikh, University of Maryland, College Park, MD 20742, USA. (milikh@astro.umd.edu)

S. L. Ossakow, Plasma Physics Division, Naval Research Laboratory, Washington, DC 20375-5346, USA. (ossakow@ccs.nrl.navy.mil)